JPSE (Journal of Physical Science and Engineering), Vol. 6, No. 2, 2021, Page 40–45.
DOI: 10.17977/um024v6i22021p040

JPSE
(Journal of Physical Science and Engineering)

http://journal2.um.ac.id/index.php/jpse
EISSN: 2541-2485

Synthesis and Characterization of Magnesium Acetate Doped $MAPbI_3$ Perovskite Solar Cells with Carbon Electrodes

Received
03 May 2021

Revised
31 May 2021

Accepted for Publication
25 June 2021

Published
04 July 2021

D A Yusra[1], N Mufti[1,2*], and E Latifah[1]

1. Department of Physics, Faculty of Mathematics and Natural Sciences, Universitas Negeri Malang, Jl. Semarang 5, Malang, 65145, Indonesia.
2. Research Centre of Advanced Materials for Renewable Energy, Universitas Negeri Malang, Jl. Semarang 5, Malang, 65145, Indonesia.

***E-mail:** nandang.mufti.fmipa@um.ac.id

Abstract
The organometal perovskite trihalide ($MAPbI_3$) based solar cell has attracted the attention of many researchers because it has the potential to be a third-generation solar cell that has high efficiency, flexibility and transparency. However, this perovskite solar cell is sensitive to the environment and less stable. In this study, a performance study of perovskite solar cells with the addition of magnesium acetate was carried out in the $MAPbI_3$ synthesis process and the use of carbon electrodes. In general, the perovskite solar cell arrangement in this study consisted of ITO/TiO_2 mp/$MAPbI_3$/carbon paste. Mesoporous TiO_2 (mp) coating was carried out using the screen printing method, while $MAPbI_3$ coating was carried out with a two-stage spin coating with the addition of magnesium acetate after PbI_2 coating in the first stage. The samples obtained were then characterized using an X-Ray Diffractometer (XRD). Analysis of the performance of solar cells was carried out by measuring I-V and photoresponses using a solar simulator. XRD results show that $MAPbI_3$ film has been formed even though there is still impurity of PbI_2. The resulting solar cell performance has a value of V_{oc} = 3.45 V and J_{sc} = 0.04 with an efficiency of around 0.09%. In the measurement of the response photo, the increase in time value was 7.29 s and the decay time was 34.38 s. The low-efficiency value is probably due to the absence of a layer of hole transfer materials (HTM) and the presence of PbI_2 impurities. However, the stability of the photoresponse pattern against time has shown quite good results even though the response is increased or the decay is slow.
Keywords: Organometal perovskite trihalide ($MAPbI_3$), perovskite solar cell, magnesium acetate, carbon electrodes, performance solar cells.

1. Introduction

Solar energy is a clean, accessible, and abundant source of energy. So far, the use of solar energy as electrical energy is still not optimal. Solar cells are devices that can convert solar energy into electrical energy directly. One type of solar cell that is on the photovoltaic market is a silicon-based solar cell. However, this solar cell has relatively low efficiency, is not transparent, and requires high technology in the manufacturing process. Therefore researchers continue to develop types of solar cells that are inexpensive, relatively simple synthesis, and high efficiency.

One of the solar cells that have received a lot of attention from researchers is the organometal perovskite trihalide ($MAPbI_3$) solar cell. This is because $MAPbI_3$ has good optoelectronic properties [1], [2], more extended electron-hole diffusion [3], high mobility [4], and low exciton binding energy [5]. In addition, $MAPbI_3$ is transparent, can be synthesized on flexible substrates, and has a high enough efficiency, which is more than 22% [6], [7].

Besides the various advantages possessed by perovskite solar cells, this solar cell also has various problems to mass-produce. One of the main problems is low stability. Several factors that influence the instability of solar cells come from the perovskite and hole transport material (HTM) used, such as Spiro-OMeTAD [8], NiO [9], PTAA [10], and P3HT [11]. This HTM layer can result in the degradation of the perovskite due to the migration of halide ions and metal ions [12]. In addition, the high cost and unstable operation of HTM are also problems in the perovskite solar cell (PSC) fabrication.

One of the efforts being developed is the fabrication of perovskite solar cells without using HTM [13] but by directly using hole extraction electrodes such as Au [14], Ni [15], or carbon [16]. Perovskite solar cell fabrication with carbon (C-PSC) has shown better stability than HTM-PSC [17]. However, magnesium acetate in the synthesis of $MAPbI_3$ and combination with carbon has not been widely studied. Therefore, in this study, perovskite solar cells doped with magnesium acetate were carried out to increase perovskite stability. Perovskite synthesis was carried out using a two-stage method with magnesium acetate in the first stage, then characterization and performance test of solar cells were carried out.

2. Method

2.1. Material

The materials used in this study were Methylamine Hydroiodide (low water content), Lead (II) Iodide (99.99% trace metals base), N, N-dimethylformamide (DMF) anhydrous, 99.8% (Sigma Aldrich), Indium glass substrate-doped tin oxide (ITO), Magnesium acetate ($MgAc_2$), ethanol, isopropyl alcohol (IPA), N, N-dimethyl sulfoxide (DMSO), Titanium Oxide (TiO_2) powder, Titanium (IV) (riethanolaminato) isoproxide, Nitric acid (HNO_3), Polyethylene glycol 6000 (PEG-6000), Triton X-100, and black conductive carbon paste.

2.2. Synthesis of CH_3NH_3I and PbI_2 Solutions

The 0.24 M of methylamine hydroiodide (CH_3NH_3I) powder was dissolved in 15 ml of isopropyl alcohol (IPA), then stirred using a magnetic stirrer at room temperature at a speed of 1000 rpm. Furthermore, the PbI_2 solution was prepared by mixing 1 M Lead (II) iodide (PbI_2) into DMF/DMSO (10/1), then stirring it on a hot plate at 100 °C (1000 rpm). The resulting PbI_2 solution is homogeneous and yellow, while the CH_3NH_3I solution is yellow and homogeneous.

2.3. Synthesis of Mesoporous TiO_2

One gram of TiO_2 powder was crushed for 15 minutes, then 0.25 g of Polyethylene glycol 6000 (PEG-6000) were added. The TiO_2 and PEG-6000 were crushed again for 30 minutes until the powder looked smoother and evenly distributed. One mililiter of nitric acid (HNO_3) and 1 drop of Triton X-100 are added to the powder resulting from grinding. Furthermore, the grinding is carried out for 10 minutes until it produces a white and even paste.

2.4. Fabrication of Perovskite Solar Cell

Indium-doped tin oxide (ITO) glass substrate was washed first with ethanol, acetone, and deionized water for 10 minutes each using an ultrasonic cleaner. Blocking layer was prepared by mixing 0.5 ml of Titanium (IV) (riethanolaminato) isoproxide into 5 ml of isopropyl alcohol (IPA), then stirring for 120 minutes at room temperature. The blocking layer solution was coated onto the ITO substrate and spin coating was carried out for 1 minute. The deposition of the mesoporous TiO_2 layer was carried out using the screen printing method, then heated at 500 °C for 30 minutes. $MgAc_2$ solution was prepared by dissolving 0.5 grams of $MgAc_2$ in 100 ml of deionized water and stirring it at room temperature for 20 minutes. The PbI_2 solution was dripped on top of ITO/TiO_2 mp and a 3000 rpm spin coating was carried out for 20 seconds, then 3 drops of $MgAc_2$ again and heated at 100 °C for 10 minutes. ITO/TiO_2 mp/PbI_2 was dripped with CH_3NH_3I solution and was done spin coating for 20 seconds then heated for 10 minutes. Deposition of PbI_2 and MAI solutions was carried out in a controlled environment with RH 50%. Carbon paste is dripped on ITO/TiO_2 mp/$MAPbI_3$ and followed by spin coating for 20 seconds (3000 rpm) then heated on a hot plate at 100 °C. The ITO/TiO_2 mp /$MAPbI_3$/carbon paste layer was successfully fabricated and then used for characterization and measurement as shown in Figure 1.

2.5. Characterization and Measurement

The XRD structure and pattern were obtained using X-Ray diffraction (XRD) from the XPERT-PRO diffractometer system. The current-voltage density curve (J-V) and the photoresponse were measured using a solar simulator under illumination of 100 mW cm^{-2} with a perovskite area of 1 cm^2.

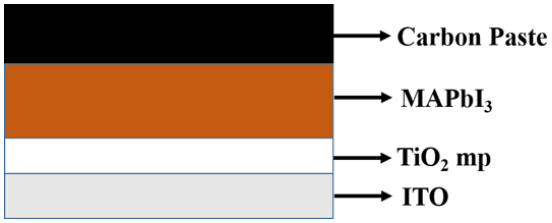

Figure 1. ITO/TiO_2 mp/$MAPbI_3$/Carbon Paste film fabrication.

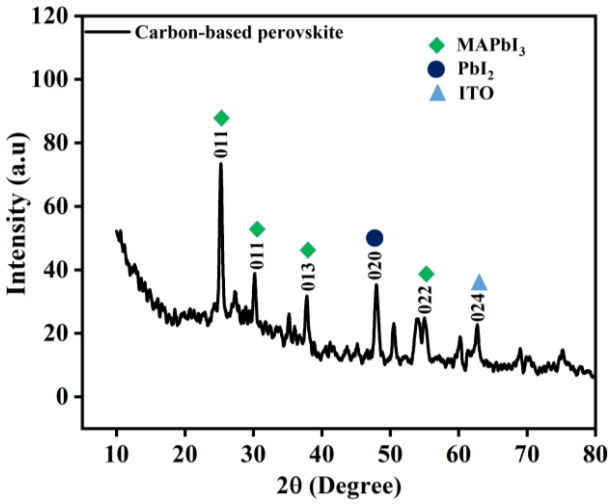

Figure 2. XRD pattern graph of ITO/TiO_2 mp/$MAPbI_3$/Carbon Paste film.

3. Result and Discussion

3.1. Analysis of X-Ray Diffraction (XRD)

The perovskite film that has been fabricated is characterized by X-Ray Diffraction (XRD) to determine the diffraction pattern of the formed crystals. Figure 2 shows that there are some of the highest peaks with field hkl, namely (001) at 25.29°, (002) at 30.11°, (013) at 37.59°, (020) at 48.07°, (022) at 53.93°, and (024) at 62.65°. The diffraction pattern above shows that there is a PbI_2 peak located at an angle of 48.07° which indicates that PbI_2 does not convert well to $MAPbI_3$ and angles other than 48.07° indicate a $MAPbI_3$ peak formed from the reaction of MAI and PbI_2. This shows that the addition of DMSO in the PbI_2 solution can slow it down crystallinity of PbI_2 [18]. In addition, the crystal size can also be obtained by using the Scherrer equation [19] with an average crystal size of 24.21 nm.

3.2. Analysis of Current Density-Voltage (J-V)

Figure 3 shows the J-V curve using commercial carbon paste as the electrode. The efficiency of perovskite solar cells obtained by measurements using a solar simulator is 0.09%. Another study using carbon electrodes also resulted in an efficiency of 7.84% with FF and J_{sc} values of 0.6% and 18.54 mA cm^{-2}, respectively [20]. The FF value generated in this study is under research [20], but the efficiency value carried out using this carbon paste is minor less than using CNT. This small efficiency predicted to have the effect of adding a layer of carbon paste as an uneven and thick electrode material. As a result, the hole displacement occurs very slowly so that the resulting efficiency is small compared to the CNT layer. The thicker the carbon layer used as the electrode material, the smaller the resulting efficiency [21]. Theoretically, the carbon paste layer as a thicker electrode affects the crystallization of $MAPbI_3$ and PbI_2 substantially, which is the infiltration rate of MAI and PbI_2 and blocks the diffusion of the PbI_2 precursor from the carbon paste layer to TiO_2 so that the filled pores become unequal [22].

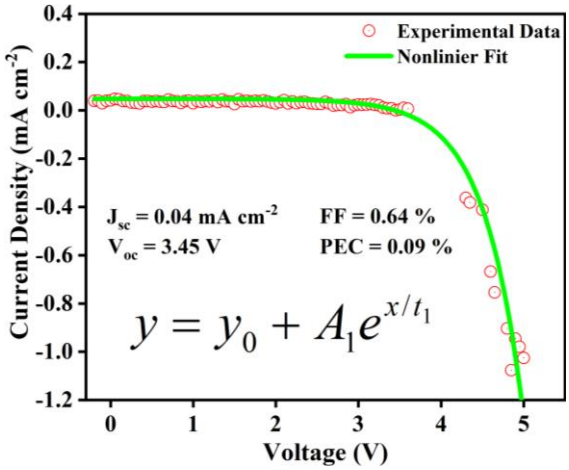

Figure 3. The J-V curve of a perovskite solar cell using carbon paste as an electrode.

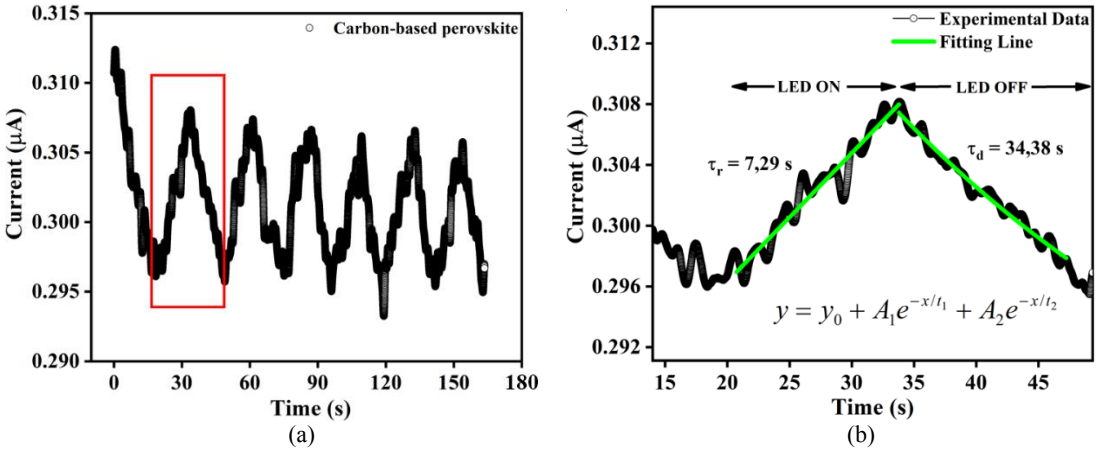

Figure 4. Graph of (a) the response of carbon-based perovskite solar cells to light and (b) Fitting of perovskite solar cell photoresponse in cycle 1 (red box).

3.3. Analysis of Photorespon

Figure 4.a shows an increase in current in the first 15 s when the solar simulator lamp is turned on and a decrease in the next 15 s when the lamp is turned off. The graph above indicates that the perovskite film has been successfully fabricated and can be applied in a photodetector with the highest and lowest current values of 0.32 μA and 0.29 μA, respectively. The value of this electric current is better than the results of other studies with a value of 0.0028 μA [23]. Figure 4.b shows a graph of the fitting between current and time with light irradiation on or off using the exponential equation [24]. Figure 4.b shows that the time increase value is 7.29 s and the decay time is 34.38 s. The increase in time of carbon-based perovskite solar cells is shorter than the time decay, this is because the light illumination in the perovskite produces electron-hole pairs so that electrons are easily excited from the conduction band to the valence band and the holes oxidize oxygen ions on the perovskite surface. When the lamp is turned off, the holes that react with oxygen ions find it difficult to escape due to the oxidation process so that it takes a long time to be oxidized [25]. Therefore, the decay time takes longer than the time when the perovskite shows the light response.

4. Conclusion

The synthesis of carbon-based perovskite thihalide ($MAPbI_3$) solar cells has been fabricated with efficiency and fill factor (FF) of 0.09% and 0.64%, respectively. Based on XRD characterization analysis and photoresponse, the crystal size was 24.21 nm and the electric current was 0.32 μA. The efficiency value is directly proportional to the thickness of the carbon paste layer as the electrode material. The carbon paste layer used is very uneven so that the resulting efficiency is small compared to a more even layer. In addition, the FF value is proportional to the addition of the carbon paste layer.

Acknowledgment
This research was supported financially by the PNBP proposal number 5.3.543/UN32.14.1/LT/2021 entitled The Effect of Magnesium Acetate Concentration ($MgAc_2$) and Humidity on the Performance of Tandem Perovskite/Silicon Solar Cells.

References

[1] J. H. Im, I. H. Jang, N. Pellet, M. Grätzel, and N. G. Park, "Growth of $CH_3NH_3PbI_3$ cuboids with controlled size for high-efficiency perovskite solar cells," *Nat. Nanotechnol.*, vol. 9, no. 11, pp. 927–932, 2014, doi: 10.1038/nnano.2014.181.

[2] S. Sun *et al.*, "The origin of high efficiency in low-temperature solution-processable bilayer organometal halide hybrid solar cells," *Energy Env. Sci*, vol. 7, no. 1, pp. 399–407, 2014, doi: 10.1039/C3EE43161D.

[3] Q. Dong *et al.*, "Electron-hole diffusion lengths >175 μm in solution-grown $CH_3NH_3PbI_3$ single crystals," *Science*, vol. 347, no. 6225, pp. 967–970, 2015, doi: 10.1126/science.aaa5760.

[4] C. S. Ponseca *et al.*, "Organometal halide perovskite solar cell materials rationalized: Ultrafast charge generation, high and microsecond-long balanced mobilities, and slow recombination," *J. Am. Chem. Soc.*, vol. 136, no. 14, pp. 5189–5192, 2014, doi: 10.1021/ja412583t.

[5] V. D'Innocenzo *et al.*, "Excitons versus free charges in organo-lead tri-halide perovskites," *Nat. Commun.*, vol. 5, no. 1, pp. 1–6, 2014, doi: 10.1038/ncomms4586.

[6] X. Li *et al.*, "A vacuum flash–assisted solution process for high-efficiency large-area perovskite solar cells," *Science*, vol. 353, no. 6294, pp. 58–62, 2016, doi: 10.1126/science.aaf8060.

[7] W. S. Yang *et al.*, "High-performance photovoltaic perovskite layers fabricated through intramolecular exchange," *Science*, vol. 348, no. 6240, pp. 1234–1237, 2015, doi: 10.1126/science.aaa9272.

[8] K. Zou *et al.*, "Phenanthrenone-based hole transport material for efficient dopant-free perovskite solar cells," *Org. Electron.*, vol. 65, pp. 135–140, 2019, doi: 10.1016/j.orgel.2018.11.015.

[9] K. Deevi and V. S. R. Immareddy, "Synthesis and characterization of optically transparent nickel oxide nanoparticles as a hole transport material for hybrid perovskite solar cells," *J. Mater. Sci. Mater. Electron.*, vol. 30, no. 6, pp. 6242–6248, 2019, doi: 10.1007/s10854-019-00927-8.

[10] Y. Kim *et al.*, "Methoxy-functionalized triarylamine-based hole-transporting polymers for highly efficient and stable perovskite solar cells," *ACS Energy Lett.*, vol. 5, no. 10, pp. 3304–3313, 2020, doi: 10.1021/acsenergylett.0c01901.

[11] P. Zhou *et al.*, "Efficient and stable mixed perovskite solar cells using P3HT as a hole transporting layer," *J. Mater. Chem. C*, vol. 6, no. 21, pp. 5733–5737, 2018, doi: 10.1039/C8TC01345D.

[12] T. A. Berhe *et al.*, "Organometal halide perovskite solar cells: degradation and stability," *Energy Environ. Sci.*, vol. 9, no. 2, pp. 323–356, 2016, doi: 10.1039/C5EE02733K.

[13] Z. Ku, Y. Rong, M. Xu, T. Liu, and H. Han, "Full printable processed mesoscopic $CH_3NH_3PbI_3/TiO_2$ heterojunction solar cells with carbon counter electrode," *Sci. Rep.*, vol. 3, no. 1, pp. 1–5, 2013, doi: 10.1038/srep03132.

[14] L. Etgar *et al.*, "Mesoscopic $CH_3NH_3PbI_3/TiO_2$ heterojunction solar cells," *J. Am. Chem. Soc.*, vol. 134, no. 42, pp. 17396–17399, 2012, doi: 10.1021/ja307789s.

[15] Z. Ku, X. Xia, H. Shen, N. H. Tiep, and H. J. Fan, "A mesoporous nickel counter electrode for printable and reusable perovskite solar cells," *Nanoscale*, vol. 7, no. 32, pp. 13363–13368, 2015, doi: 10.1039/C5NR03610K.

[16] Z. Wei *et al.*, "Cost-efficient clamping solar cells using candle soot for hole extraction from ambipolar perovskites," *Energy Env. Sci*, vol. 7, no. 10, pp. 3326–3333, 2014, doi: 10.1039/C4EE01983K.

[17] Z. Wei *et al.*, "A multifunctional C+ epoxy/Ag paint cathode enables efficient and stable operation of perovskite solar cells in watery environments," *J. Mater. Chem. A*, vol. 3, no. 32, pp. 16430–16434, 2015, doi: 10.1039/C5TA03802B.

[18] W. Li, J. Fan, J. Li, Y. Mai, and L. Wang, "Controllable grain morphology of perovskite absorber film by molecular self-assembly toward efficient solar cell exceeding 17%," *J. Am. Chem. Soc.*, vol. 137, no. 32, pp. 10399–10405, 2015, doi: 10.1021/jacs.5b06444.

[19] F. Acosta-Humánez, O. Almanza, and C. Vargas-Hernández, "Effect of sintering temperature on the structure and mean crystallite size of $Zn_{1-x}Co_xO$ (x= 0.01-0.05) samples," *Superf. Vacío*, vol. 27, no. 2, pp. 43–48, 2014.

[20] C. V. V. M. Gopi, M. Venkata-Haritha, K. Prabakar, and H. J. Kim, "Low-temperature easy-processed carbon nanotube contact for high-performance metal- and hole-transporting layer-free perovskite solar cells," *J. Photochem. Photobiol. Chem.*, vol. 332, pp. 265–272, 2017, doi: 10.1016/j.jphotochem.2016.09.003.

[21] L. Fagiolari and F. Bella, "Carbon-based materials for stable, cheaper and large-scale processable perovskite solar cells," *Energy Environ. Sci.*, vol. 12, no. 12, pp. 3437–3472, 2019, doi: 10.1039/C9EE02115A.

[22] Y. Rong *et al.*, "Hole-conductor-free mesoscopic $TiO_2/CH_3NH_3PbI_3$ heterojunction solar cells based on anatase nanosheets and carbon counter electrodes," *J. Phys. Chem. Lett.*, vol. 5, no. 12, pp. 2160–2164, 2014, doi: 10.1021/jz500833z.

[23] J. Zheng *et al.*, "Spin-coating free fabrication for highly efficient perovskite solar cells," *Sol. Energy Mater. Sol. Cells*, vol. 168, pp. 165–171, 2017, doi: 10.1016/j.solmat.2017.04.029.

[24] N. Mufti *et al.*, "Photoelectrochemical performance of ZnO nanorods grown on stainless steel substrate," in *IOP Conf. Ser. Mater. Sci. Eng.*, vol. 515, no. 1, 2019, p. 012023, doi: 10.1088/1757-899X/515/1/012023.

[25] S. Dhara and P. K. Giri, "ZnO nanowire heterostructures: Intriguing photophysics and emerging applications," *Rev. Nanosci. Nanotechnol.*, vol. 2, no. 3, pp. 147–170, 2013, doi: 10.1166/rnn.2013.1032.